2356–2367 Nucleic Acids Research, 2007, Vol. 35, No. 7 Published online 27 March 2007
doi:10.1093/nar/gkm143

RNase T1 mimicking artificial ribonuclease

N. L. Mironova, D. V. Pyshnyi, D. V. Shtadler, A. A. Fedorova, V. V. Vlassov and M. A. Zenkova*

Institute of Chemical Biology and Fundamental Medicine SB RAS, Lavrentiev Ave., 8, Novosibirsk, Russia, 630090

Received December 21, 2006; Revised February 5, 2007; Accepted February 22, 2007

ABSTRACT

Recently, artificial ribonucleases (aRNases)—conjugates of oligodeoxyribonucleotides and peptide $(LR)_4$-G-amide—were designed and assessed in terms of the activity and specificity of RNA cleavage. The conjugates were shown to cleave RNA at Pyr-A and G–X sequences. Variations of oligonucleotide length and sequence, peptide and linker structure led to the development of conjugates exhibiting G–X cleavage specificity only. The most efficient catalyst is built of nonadeoxyribonucleotide of unique sequence and peptide $(LR)_4$-G-NH_2 connected by the linker of three abasic deoxyribonucleotides (conjugate *pep*-9). Investigation of the cleavage specificity of conjugate *pep*-9 showed that the compound is the first single-stranded guanine-specific aRNase, which mimics RNase T1. Rate enhancement of RNA cleavage at G–X linkages catalysed by *pep*-9 is 10^8 compared to non-catalysed reaction, *pep*-9 cleaves these linkages only 10^5-fold less efficiently than RNase T1 ($k_{cat\_RNase\ T1}/k_{cat\_pep\text{-}9} = 10^5$).

INTRODUCTION

The major challenges in the development of artificial ribonucleases (aRNases) are the achievement of sequence specificity of RNA cleavage and high cleavage efficiency. Natural ribonucleases of RNase A family (1–4) exhibit pyrimidine-X specificity. Ribonucleases of T1 family (RNase T1 from *Aspergillus oryzae* (5) and RNase F1 from *Fusarium moniliforme* (6) exhibit guanine-X specificity, and RNase U2 from *Ustilago sphaerogena* (7) exhibit adenine-X specificity. Attempts have been made to alter the specificity of ribonuclease T1 by protein engineering methods (8), but this goal has not been achieved till date.

One approach to the design of aRNases consists of mimicking active sites of natural enzymes by conjugates bearing the functional groups of amino acids that form the catalytic centre of the enzyme and catalysing the transesterification reaction [for example, imidazole (9–11), aminogroups (12), guanidinium groups (13)]. aRNases designed using this approach usually display cleavage specificity similar to that of RNase A: they cleave RNA predominantly at linkages within Pyr-A motifs, which are known to be highly sensitive towards various cleaving agents (14). These aRNases accelerate cleavage at the most sensitive sites within RNA.

The sequence specificity of natural RNases is determined by the substrate recognition centre in which the specific interaction of amino acids with RNA provides for the specific binding and placement of a particular heterocyclic base, thus resulting in the optimal conformation of internucleotide phosphodiester bonds, which are subjected to cleavage. Accurate mimicking of ribonuclease active centres is a difficult task because of their complex spatial structure providing for multipoint contacts within the enzyme–substrate complex, and specific and dynamic nature of the centres that undergo conformational changes.

Attempts were made to stabilize the RNA heterocyclic bases optimally for cleavage conformations via stacking interactions with aromatic amino acids [for example, phenylalanine (15)], which were introduced into the structure of conjugates mimicking RNase active centres. However, these conjugates did not exhibit any cleavage specificity other than Pyr-A. aRNases displaying other specificity were developed by introducing guanidinium groups and arginine residues into the structure of aRNases: some G–X cleavage activity was reported for conjugates of anthraquinone and imidodiacetate bearing carboxylic and ammonium ions (13) and conjugates of oligodeoxyribonucleotides and peptide $(LR)_4$-G-amide (16–21).

Recently, the conjugates of peptide $(LR)_4$-G-NH_2 attached to 5′-terminal phosphate of antisense oligonucleotides were obtained (16,19). These conjugates were found to cleave RNA both in the vicinity of oligonucleotide complementary sequence and in a random manner at Pyr-A and G–X linkages (16,19). We found that the oligonucleotide in the conjugates plays an unusual role: it promotes formation of an 'active' peptide conformation because the peptide itself exhibits no ribonuclease activity (17,20). All designed oligonucleotide–peptide conjugates

*To whom correspondence should be addressed. Tel: (383)3333761; Fax: (383)3333677; Email: marzen@niboch.nsc.ru

displayed either G–X > Pyr-A or G–X < Pyr-A activity, but both activities were observed simultaneously. The main task of this work was to design the conjugate(s) exhibiting G–X cleavage activity similar only to RNase T1.

In this article, we solve this problem and describe the first single-stranded guanine-specific aRNase—conjugate of nonadeoxyribonucleotide GGATCTCTT and peptide $(RL)_4$-G-amide connected by the linker of three deoxyribose residues (*pep*-**9**), which display only G–X cleavage activity under various conditions. Rate enhancement of RNA cleavage at G–X linkages catalysed by *pep*-**9** is 10^8, as compared to non-catalysed reactions; *pep*-**9** cleaves G–X linkages only 10^5-fold less rapidly than RNase T1 ($k_{cat\_RNase\ T1}/k_{cat\_pep\text{-}9} = 10^5$).

MATERIALS AND METHODS

[γ-^{32}P]ATP (specific activity >3000 Ci/mM) was from Biosan Co. T4 polynucleotide kinase and RNase T1 were purchased from Fermentas (Lithuania). Peptide $(LR)_4$-G-NH_2 was purchased from Diapharm Ltd. (St. Petersburg, Russia). Fok I restriction endonuclease was from Sibenzyme (Russia). T7 RNA-polymerase was prepared by Dr V. Ankilova (this institute). All buffers were prepared using MilliQ water, contained 0.1 mM EDTA and were filtered through 0.22-μm millipore filters.

Oligonucleotides

Oligoribonucleotides $^{5'}$AGAAACAACGGUUCGGAAG UU$^{3'}$ (RNA-21*s*) and $^{5'}$CUAACUUCCGAACCGUU GUUU$^{3'}$ (RNA-21*as*), the chimeric ribo/2′-*O*-methylribo oligonucleotides $^{5'}$UUC AUrG∼UAAA$^{3'}$ (RNA-10$_{\mathbf{rGU}}$), $^{5'}$UUCAUrG∼AAAA$^{3'}$ (RNA-10$_{\mathbf{rGA}}$), $^{5'}$UUCAUrG∼GAAA$^{3'}$ (RNA-10$_{\mathbf{rGG}}$) and $^{5'}$UUCAUrG∼CAAA$^{3'}$ (RNA-10$_{\mathbf{rGC}}$) were chemically synthesized by standard protocols. 2′-*O*-Methylribo units are underlined.

Oligodeoxyribonucleotides (pdRib)$_3$-$^{5'}$pGGATCTCTT$^{3'}$, $^{5'}$pGGATCTCTT^{3}, (pdRib)$_3$-$^{5'}$pGGATCTCTA$^{3'}$, (pdRib)$_3$-$^{5'}$pTCTCTC$^{3'}$, $^{5'}$pTCTCTC$^{3'}$, (pdRib)$_3$-$^{5'}$pTCT CTT$^{3'}$, (pdRib)$_3$-$^{5'}$pGGGATCTCTT$^{3'}$, (pdRib)$_3$-$^{5'}$pGAT CTCTT^{3}, (pdRib)$_3$-$^{5'}$pGGA-(pdRib)$_4$-T$^{3'}$ and (pdRib)$_3$-$^{5'}$pGGAT$^{3'}$ were synthesized by the standard phosphoramidite protocol on ASM-700 synthesizer (Biosset, Russia) using solid support, nucleoside phosphoramidites, dSpaser (pRib), chemical phosphorylation reagent from Glenn Research (USA). Oligonucleotides were isolated by consecutive ion-exchange (Polysil SA-500 columns, Russia) and reverse-phase HPLC (LiChrosorb RP-18 columns, Merck, Germany) according to standard protocols.

Preparation of conjugate pep-9

Conjugates NH_2-G-$(RL)_4$-(pdRib)$_3$-$^{5'}$pGGATCTCTT$^{3'}$ (*pep*-**9**), NH_2-G-$(RL)_4$-$^{5'}$pGGATCTCTT^{3} (*pep*-**9**$^{(-L)}$), NH_2-G-$(RL)_4$-(pdRib)$_3$-$^{5'}$pGGATCTCTA$^{3'}$ (*pep*-**9**$^{(T/A)}$), NH_2-G-$(RL)_4$-(pdRib)$_3$-$^{5'}$pTCTCTC$^{3'}$ (*pep*-**(TC)$_3$**), NH_2-G-$(RL)_4$-$^{5'}$pTCTCTC$^{3'}$ (*pep*-**(TC)$_3$**$^{(-L)}$), NH_2-G-$(RL)_4$-(pdRib)$_3$-$^{5'}$pTCTCTT$^{3'}$ (*pep*-**TCTCTT**), NH_2-G-$(RL)_4$-(pdRib)$_3$-$^{5'}$pGGGATCTCTT$^{3'}$ (*pep*-**9**$^{(+5'G)}$), NH_2-G-$(RL)_4$-(pdRib)$_3$-$^{5'}$pGATCTCTT$^{3'}$ (*pep*-**9**$^{(-5'G)}$), NH_2-G-$(RL)_4$-(pdRib)$_3$-$^{5'}$pGGA-(pdRib)$_4$-T$^{3'}$ (*pep*-**GGA(pdRib)$_4$T**) and NH_2-G-$(RL)_4$-(pdRib)$_3$-$^{5'}$pGGAT$^{3'}$ (*pep*-**GGAT**) were synthesized by the formation of phosphamide bond between 5′-terminal phosphate of deoxyribose linker or 5′-phosphate group and N-terminal α-amino group of oligopeptide according to published protocol (22). The conjugates were isolated by reverse-phase HPLC on LiChrosorb RP-18 column (4 × 250 mm). Homogeneity of the conjugates was tested by electrophoresis in 15% polyacrylamide/8 M urea gel followed by staining with 'Stains-all'. The homogeneity of the conjugates was 95–98%. The structure and properties of the conjugate *pep*-**9** are protected by patent (23).

MALDI-TOF mass spectrometry

Molecular weights of peptides, oligonucleotides and conjugate *pep*-**9** have been verified by MALDI-TOF mass spectrometry on a REFLEX III mass spectrometer equipped with a pulsed nitrogen laser emitting at 337.1 nm (Bruker Daltonics, Germany). An overlayer preparation was used with a 3-hydroxypicolinic acid (HPA) or 2,5-dihydroxybenzoic acid (DHB) as matrix. A 10:1 mixture 50 mg/ml matrix in aqueous acetonitrile (1:1 v/v), and 100 mg/ml aqueous ammonium citrate was spotted in 1 μL aliquots on a bed and dried. Here, 1 μl 10 μM aqueous solution of a sample was added. MALDI-TOF mass spectra were acquired in positive- or negative-ion mode. Samples were analysed in reflector mode using an accelerating voltage of 20 kV. All spectra were the result of signal averaging 200 laser shots. Calibrations were performed in accordance with the manufacturer's recommendations. For oligonucleotides, peptide and conjugate *pep*-**9** expected and measured masses were: (pdRib)$_3$-GGATCTCTT expected 3326.1, measured 3326.73, a [M+H]+; peptide $(LR)_4$-G-NH_2 expected 1151.78, measured 1151.81, m [M+H]+; conjugate *pep*-**9** expected 4459.6, measured 4459.03, a [M+H]+; conjugate *pep*-**9**$^{(-L)}$ expected 3919.2, measured 3922.55, a [M+H]+; where a, m refers to average and monoisotopic mass, respectively.

Preparation of [5′-^{32}P]-labelled RNA substrates

A 96-nt fragment of RNA HIV-1 (RNA-96) was prepared by *in vitro* transcription using T7 RNA polymerase and Fok I—linearized plasmid pHIV-1 as described in (17).

RNA-96 was dephosphorylated using bacterial alkaline phosphatase (BAP) according to described protocol (24). The reaction mixture, 50 μl of 50 mM Tris-HCl, pH 8.5, containing 1 mM EDTA, 0.2% SDS, 2% formamide, 2.5 mM DTT, 0.1 OD of RNA-96 and 2 U of BAP was incubated at 37°C for 1 h. After 30 min, BAP was added again to the reaction mixture. The reaction was quenched by phenol:chloroform (1:1, v/v) extraction, followed by extraction with ethyl ester and precipitation with ethanol.

5′-End labelling of chimeric ribo/2′-*O*-methylribo oligonucleotides (RNA-21$_{\mathbf{rGX}}$, where X refers to A, U, G or C), RNA-21*s* and RNA-96 were carried out using

[γ^{32}P]ATP and T4 polynucleotide kinase according to (24). [^{32}P]-Labelled RNA was isolated by electrophoresis in 12% PAAG/8 M urea gel. RNA was visualized by autoradiography on an X-ray film. [^{32}P]-Labelled RNA-21 and RNA-96 were eluted from the gel by 300 µl of 0.3 M sodium acetate, pH 5.5, and precipitated with ethanol.

Ribonuclease activity assay

The reaction mixture (10 µl) contained 50 000 c.p.m. [^{32}P]-labelled RNA-96, one of the conjugates *pep*-**9**, *pep*-**9**$^{(-L)}$, *pep*-**9**$^{(T/A)}$, *pep*-**(TC)$_3$**, *pep*-**(TC)$_3$**$^{(-L)}$, *pep*-**TCTCTT**, *pep*-**9**$^{(+5'G)}$, *pep*-**9**$^{(-3'G)}$, *pep*-**GGA(pdRib)$_4$T**, *pep*-**GGAT** at a concentration ranging from 10 to 50 µM, 50 mM Tris-HCl, pH 7.0, 0.2 M KCl, 1 mM EDTA and 100 µg/ml total RNA carrier (total tRNA from *Escherichia coli*). The mixtures were incubated at 37°C for 3–8 h and quenched by precipitation of RNA with 2% lithium perchlorate in acetone (150 µl). RNA was collected by centrifugation and dissolved in loading buffer (6 M urea, 0.025% bromophenol blue, 0.025% xylene cyanol). RNA and RNA cleavage products were resolved in 12% PAAG/8 M urea gel using TBE (100 mM Tris-borate, pH 8.3, 2 mM EDTA) as running buffer. To identify cleavage sites, an imidazole ladder and G-ladder produced by partial RNA cleavage with 2 M imidazole buffer (pH 7.0) (25) and with RNase T1 (26), respectively, were run in parallel. Quantitative data were obtained by counting using Molecular Imager (BioRad). The total extent of RNA cleavage and the extent of RNA cleavage at specific sites were determined as a ratio of radioactivity measured in the RNA fragment(s) to the total radioactivity applied onto the gel.

Effective rate constants of spontaneous RNA cleavage. The reaction mixtures (100 µl) containing 500 000 c.p.m. [^{32}P]-labelled RNA-10$_{rGU}$, RNA-10$_{rGA}$, RNA-10$_{rGG}$ or RNA-10$_{rGC}$ and corresponding RNA at a concentration of 0.1 µM, 50 mM Tris-HCl, pH 7.0, 1 mM EDTA, were incubated at temperatures from 50 to 80°C for 10 min–9 h. At various time points, aliquots were taken, frozen at −70°C for 10 min and stored at −20°C. RNA cleavage products were analysed in 12% PAAG/8 M urea gel as described above.

Effective rate constants of spontaneous cleavage at G–X motifs, (k_{eff}), were obtained by fitting data to the single exponential Equation (1) (27):

$$P_t = P_\infty \cdot (1 - \exp -k_{eff} \cdot t), \quad \mathbf{1}$$

where P_t and P_∞ are the fraction of substrate cleaved at time t and at the end point, respectively.

Effective rate constants of spontaneous RNA cleavage at 37°C were obtained by extrapolation to 37°C data of Arrhenius plot ln(k_{eff}) to 1/T.

Effective rate constants of RNA cleavage by pep-9 and RNase T1. The reaction mixtures (10 µl) containing 50 000 c.p.m. [^{32}P]-labelled RNA-10$_{rGU}$, RNA-10$_{rGA}$, RNA-10$_{rGG}$ or RNA-10$_{rGC}$ and the corresponding RNA at a concentration of 0.1 µM, 5–10 µM *pep*-**9** or 0.5–1 U RNase T1, 50 mM Tris-HCl, pH 7.0, 1 mM EDTA, were incubated at 37°C for 10–99 h and 5–90 min, respectively. At particular time, reaction mixtures were frozen at –70°C for 10 min and then stored at –20°C. RNA cleavage products were analysed in 12% PAAG/8 M urea gel as described above. Effective rate constants, (k_{eff}), were obtained by fitting data to the single exponential Equation (1).

Salt concentration profile

Cleavage of RNA-96. Cleavage reactions were performed in the reaction mixture (10 µl) containing 50 000 c.p.m. [5′-^{32}P]-RNA-96, 10 µM *pep*-**9**, 50 mM Tris-HCl, pH 7.0, LiCl at concentration ranging from 0 to 500 mM, 1 mM EDTA, 100 µg/ml RNA carrier. The mixtures were incubated at 37°C for 5–8 h, and reactions were quenched by RNA precipitation with 150 µl of 2% lithium perchlorate in acetone followed by the analysis of cleavage products as described above.

Cleavage of RNA-10$_{rGG}$. Cleavage reactions were performed in the reaction mixture (10 µl) containing 50 000 c.p.m. [5′-^{32}P]-RNA-10$_{rGG}$ (10^{-7} M), 10 µM *pep*-**9**, 50 mM Tris-HCl, pH 7.0, 1 mM EDTA, LiCl at a concentration of 0–200 mM or $MgCl_2$ at a concentration of 0–20 mM. The mixtures were incubated at 37°C for 52 h. Reactions were quenched by dilution with 8 M urea containing leading dyes, and cleavage products were analysed by electrophoresis in 15% PAAG/8 M urea gel as described above.

pH profile of ribonuclease activity of pep-9 and RNase T1

pH profile of RNA cleavage by the conjugate *pep*-**9** and RNase T1 was assayed in experiments with RNA-96 at pH from 6.0 to 9.5. The buffers were: 50 mM bis-tris-propane-KOH for pH 6.0–9.5; 50 mM Tris-HCl for pH 7.0–9.0; 50 mM MES-HCl for pH 5.5–6.0; 50 mM sodium acetate–CH_3COOH for pH 3.7–5.0. All buffers contained 200 mM KCl and 1 mM EDTA.

pH profile of RNase T1 activity. Reactions were performed in reaction mixtures (10 µl) containing 50 000 c.p.m. [5′-^{32}P]-RNA-96, 1.5–3 U of RNase T1, one of the buffers supplemented with 100 µg/ml RNA carrier at 37°C for 15 min. Reactions were quenched by dilution with 40 µl of 0.3 M sodium acetate, pH 5.5, supplemented with 1 µg of RNA carrier followed by phenol:chloroform extraction (1:1, v/v) and ethanol precipitation.

pH profile of pep-9 activity. Reactions were performed in reaction mixtures (10 µl) containing 50 000 c.p.m. [5'-^{32}P]-RNA-96, 20 µM of *pep*-**9**, one of the buffers supplemented with 100 µg/ml RNA carrier at 37°C for 3–6 h. Reactions were quenched by RNA precipitation with 150 µl of 2% lithium perchlorate in acetone. RNA cleavage products were analysed in 12% PAAG/8 M urea gels as described above.

Structure specificity assay

In these experiments, 21-mer ribooligonucleotide RNA-21*s* and/or the duplex formed by RNA-21*s* with complementary strand RNA-21*as* were used as substrates.

Duplex formation. Reaction mixture (8 μl) containing a mixture of [5′-^{32}P]-RNA-21*s* and RNA-21*s* at a concentration of 8 μM (400 000 c.p.m., Cherenkov counting), equimolar amount of RNA-21*as*, 50 mM Tris-HCl, pH 7.0, 0.2 M KCl, 1 mM EDTA, was incubated at 80°C for 1 min and then slowly cooled to room temperature for 1.5 h. Formation of the duplex RNA-21*s*/RNA-21*as* was monitored by electrophoresis in 10% native PAAG.

Cleavage reaction. Reaction mixture (10 μl) contained 50 000 c.p.m. [5′-^{32}P]-RNA-21*s* (0.1 μM) or RNA-21s–RNA-21*as* duplex (0.1 μM), 5 μM of conjugate *pep*-**9**, 50 mM Tris-HCl, pH 7.0, 200 mM KCl, 1 mM EDTA. Mixtures were incubated at 37°C for 1–24 h, and the reaction was quenched by precipitation with ethanol in the presence of 0.3 M sodium acetate, pH 5.5, supplemented with 1 μg RNA carrier. Products of RNA cleavage were analysed in 12% PAAG/8 M urea gel.

Probing of RNA-96 structure by conjugate *pep*-9 and RNase T1

Probing of RNA-96 structure by conjugate *pep*-**9** and RNase T1 was carried out under native (buffer *n*), semi-denaturing (buffer *s*/*d*) and denaturing (buffer *d*, *d1* and *d2*) conditions: *n* (50 mM Tris-HCl, pH 7.0, 200 mM KCl, 5 mM $MgCl_2$, 1 mM EDTA); *s*/*d* (50 mM Tris-HCl, pH 7.0, 200 mM KCl, 1 mM EDTA); *d* (6 M urea, 25 mM sodium citrate, pH 4.5–4.8, 1 mM EDTA); *d1* (6 M urea, 50 mM Tris-HCl, pH 7.0, 1 mM EDTA); *d2* (50 mM Tris-HCl, pH 7.0, 1 mM EDTA).

Probing by RNase T1. Reaction mixture (10 μl) contained 50 000 c.p.m. [^{32}P]-labelled RNA-96, 3–5 U RNase T1 and one of the buffers *d*, *d1*, *d2*, *s*/*d* or *n* supplemented with 100 μg/ml RNA carrier. The mixtures in buffer *d* were incubated at 55°C for 10 min, while the mixtures containing other buffers were incubated at 37°C for 10 min. The reaction in buffer *d* was quenched by the addition of 2 μl of Tris-borate buffer, pH 8.3. The reactions in buffers *d1*, *d2*, *s*/*d* and *n* were quenched by the precipitation of RNA with 150 μl of 2% lithium perchlorate in acetone. RNA cleavage products were analysed in 12% PAAG/8 M urea gel as described above.

Probing by pep-9. Reaction mixtures (10 μl) contained 50 000 c.p.m. [^{32}P]-labelled RNA-96, 10 μM conjugate *pep*-**9**, and one of the buffers—*d1*, *d2*, *s*/*d* or *n* supplemented with 100 μg/ml RNA carrier. The mixtures were incubated at 37°C for 3–5 h, and the reaction was quenched by the precipitation of RNA with 150 μl of 2% lithium perchlorate in acetone. RNA cleavage products were analysed in 12% PAAG/8 M urea as described above.

RESULTS

Design of the conjugate pep-9

By screening experiments in which oligonucleotide and peptide fragments of the conjugates were systematically varied (18), the conjugate displaying RNase T1 cleavage specificity was identified. The conjugate consists of nonadeoxyribonucleotide GGATCTCTT and peptide $(LR)_4$-G-amide, N-terminus of which is attached to the 5′-terminus of oligonucleotide via the linker group built of three deoxyribose residues. The conjugate *pep*-**9** was synthesized as described in (22) via the formation of phosphamide bond between 5′-terminal phosphate of the oligonucleotide analogue $(pdRib)_3$-pGGATCTCTT and α-amino group of N-terminal leucine residue of the peptide.

To elucidate structure–function relationships in the conjugate *pep*-**9**, a series of *pep*-**9** analogues containing modifications in the oligonucleotide sequence and linker structure were synthesized and studied in parallel with *pep*-**9** (Figure 1).

Ribonuclease activity of pep-9 and specificity of RNA cleavage

Ribonuclease activity of the conjugates was tested in experiments with the following RNAs: *in vitro* transcript of 96-nt fragment of HIV-1 RNA comprising the primer-binding site (hereafter RNA-96), synthetic oligoribonucleotide RNA-21*s* (21 nt long), duplex RNA-21*s*/RNA-21*as* (19 bp) and a series of chimeric ribo/2′-*O*-methylribo oligonucleotides (10 nt long), each containing only one ribo-linkage G–U, G–A, G–G or G–C (2′-*O*-methylribonucleotides are underlined).

Ribonuclease activity and specificity of RNA cleavage by *pep*-**9** and its analogues were studied in experiments with RNA-96 containing 21 G–X linkages. 5′-End-labelled RNA-96 was incubated with *pep*-**9**, and the cleavage products were identified (Figure 2A). Conjugate *pep*-**9** cleaved RNA-96 only at linkages in G–X motifs. The total extent of RNA-96 cleavage by the conjugate *pep*-**9** was 60% (at conjugate concentration 50 μM) after 8 h of incubation, and the entire RNA-96 cleavage was achieved within 18 h. Under the conditions used, RNA cleavage at Pyr-A linkages did not exceed the level of spontaneous RNA hydrolysis at these motifs in the controls.

RNA-96 was cleaved by *pep*-**9** at linkages within all 21 G–X motifs (Figure 2A and B). According to intensity and time of appearance of cleavage products, the cleavage sites can be divided in two groups: the primary sites, where strong cuts are observed (Figure 2B, enclosed by red), and secondary sites, where weak cleavages appeared after longer incubation (Figure 2B, enclosed by yellow). Strong cuts are located in the single-stranded regions or regions with unstable secondary structure, while weak cuts are observed in the double-stranded regions (28).

To study the structure specificity of *pep*-**9** and to exclude the possibility of structure breathing under the condition used (absence of Mg^{2+}, 37°C) ribooligonucleotide RNA-21*s* and duplex formed by RNA-21*s* with its complementary strand RNA-21*as* were subjected to cleavage by this

Peptide	Linker group	Oligonucleotide 5′ ⟶ 3′	Conjugate
	-(pdRib)$_3$-	pGGATCTCTT	*pep*-**9**
NH_2-G-(RL)$_4$-	–	pGGATCTCTT	*pep*-**9**$^{(-L)}$
	-(pdRib)$_3$-	pGGATCTCTA	*pep*-**9**$^{(T/A)}$
	-(pdRib)$_3$-	pGGGATCTCTT	*pep*-**9**$^{(+5'G)}$
	-(pdRib)$_3$-	pGATCTCTT	*pep*-**9**$^{(-5'G)}$
	-(pdRib)$_3$-	pTCTCTC	*pep*-**(TC)$_3$**
	–	pTCTCTC	*pep*-**(TC)$_3$**$^{(-L)}$
	-(pdRib)$_3$-	pTCTCTT	*pep*-**TCTCTT**
	-(pdRib)$_3$-	pGGA-(pdRib)$_4$-T	*pep*-**GGA-(pdRib)$_4$-T**
	-(pdRib)$_3$-	pGGAT	*pep*-**GGAT**

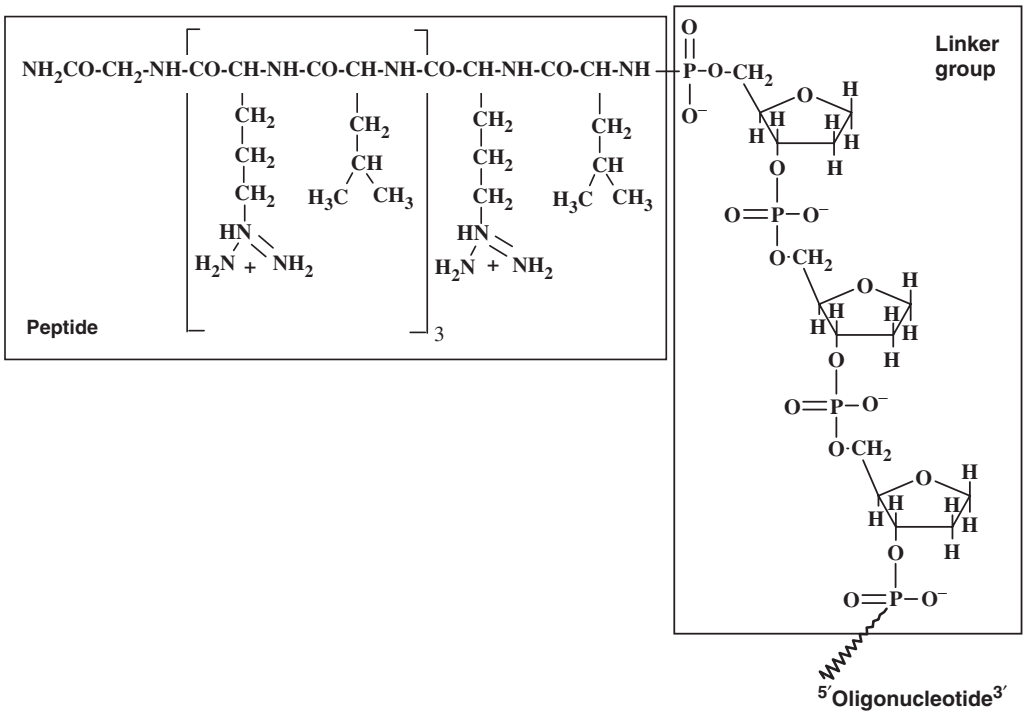

Figure 1. Structures of oligonucleotide–peptide conjugates. The conjugate *pep*-**9** is marked.

catalyst (Figure 3A). Single-stranded substrate RNA-21*s* was efficiently cleaved by *pep*-**9**. Products of the cleavage at linkages after G_2, G_{10}, G_{11}, G_{15}, G_{16} and G_{19} were similar to that produced by RNase T1. Longer incubation (up to 24 h) did not affect the pattern of RNA-21*s* cleavage, and no other cuts appeared. On the contrary, double-stranded duplex RNA-21*s*–RNA-21*as* was entirely resistant to *pep*-**9**. Even upon long incubation of the duplex (up to 48 h) in the presence of *pep*-**9**, no cuts were observed, showing that *pep*-**9** is a single-stranded aRNase displaying RNase T1-like specificity of cleavage (Figure 3B).

Kinetic parameters and the effect of pep-9 concentration on RNA cleavage

The effect of *pep*-**9** concentration on RNA cleavage was studied using RNA-96 as a substrate (Figure 2C). The curve has a shape with saturation similar to the curves of other oligonucleotide–peptide conjugates studied previously (17). This type of curve characterizes cleavage reaction proceeding within a complex, which is an attribute of enzymatic reactions. At a *pep*-**9** concentration of 30 μM, the curve reached a plateau (cleavage extent 65%), where cleavage occurred only at linkages in G–X motifs. Further increase of conjugate concentration resulted neither in the increase of cleavage extent nor in the appearance of new cleavage sites and specificity other than G–X.

Effective rate constants of RNA cleavage by *pep*-**9** at individual G–X linkages were measured in experiments with chimeric ribo/2′-*O*-methylribo oligonucleotides (10 nt long) containing only one ribo-linkage G–U (RNA-10$_{rGU}$), G–A (RNA-10$_{rGA}$), G–G (RNA-10$_{rGG}$) or G–C (RNA-10$_{rGC}$). To compare the rates of cleavage at G–X motifs observed in the presence of *pep*-**9** and rates of

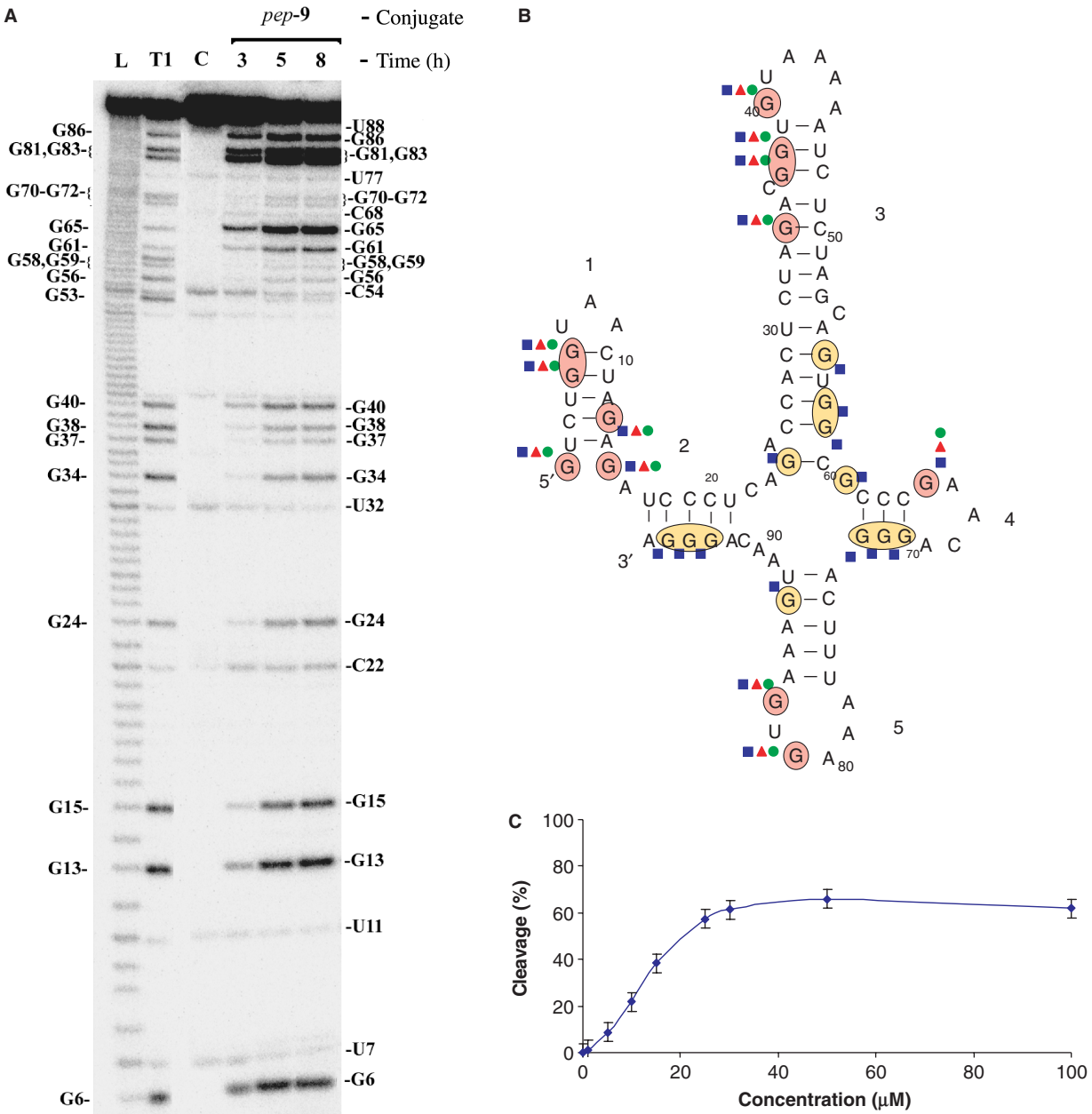

Figure 2. (**A**) Ribonuclease activity of *pep*-**9**. Autoradiograph of 12% polyacrylamide–8M urea gel. Lanes L and T1—imidazole ladder and partial RNA digestion with RNase T1 under denaturing conditions. Lane C—RNA incubated in the absence of the conjugate for 8 h. Lanes 3, 5 and 8—[5′-^{32}P]-RNA-96 was incubated in the presence of 10 μM *pep*-**9** at 37°C for 3, 5 and 8 h, respectively. Sites of RNA cleavage by RNase T1 and conjugate *pep*-**9** are shown on the left and right, respectively. (**B**) Secondary structure of RNA-96 [as determined by C. Isel *et al.* (28)] and sites of cleavage by *pep*-**9** under different conditions. Guanine residues showed by red correspond to primary sites cleaved by *pep*-**9** under standard conditions (50 mM Tris-HCl, pH 7.0, 0.2 M KCl, 1 mM EDTA), guanine residues showed by yellow correspond to secondary sites cleaved by *pep*-**9** under standard conditions. Standard conditions correspond to semi-denaturing conditions. Blue squares, red triangles and green circles indicate linkages cleaved by *pep*-**9** under denaturing (buffer *d*2), semi-denaturing (buffer *s*/*d*) and native conditions (buffer *n*), respectively. For buffers, see the Materials and methods section. (**C**) The effect of *pep*-**9** concentration on cleavage of RNA-96. Assay conditions: [5′-^{32}P]-RNA-96 was incubated in the presence of *pep*-**9** in 50 mM Tris-HCl buffer, pH 7.0, containing 0.2 M KCl, 1 mM EDTA, 100 μg/ml RNA carrier, at 37°C for 8 h.

spontaneous hydrolysis of these linkages, the cleavage of chimeric ribooligonucleotides was performed in the absence of any catalyst at temperatures ranging from 50 to 80°C. Effective rate constants of spontaneous RNA hydrolysis (k_{eff_nc}) at 37°C were obtained by extrapolation to 37°C data of Arrenius plot ln(k_{eff}) versus $1/T$. The k_{cat} of RNA cleavage by *pep*-**9** was calculated using the equation $k_{eff} = k_{cat} \cdot [E]$ (Table 1), and the k_{cat} of spontaneous hydrolysis was assumed to be k_{eff}. It is seen that cleavage by *pep*-**9** at linkage G–G proceeds at the highest rate: k_{cat} for G–G is $1.27\,M^{-1}s^{-1}$. Cleavage at the linkages G–A and G–C proceeds at similar rates ($k_{cat} = 0.50\,M^{-1}s^{-1}$). Linkage G–U is the most resistant to cleavage. Rates of spontaneous hydrolysis of G–A and G–C linkages were the highest among G–X motifs and have similar values (see Table 1). Rate of spontaneous hydrolysis of G–G linkage is lower ($k_{cat} = 1.35 \times 10^{-8}\,s^{-1}$), while linkage G–U also displays enhanced resistance towards spontaneous hydrolysis. Rate enhancement for *pep*-**9** can be calculated as a ratio of rate constants of catalysed to non-catalysed reactions ($k_{cat\_pep\text{-}9}/k_{cat\_nc}$) for each particular ribo-linkage that is on an average 2×10^7–10^8. Rate constants (k_{cat}) for cleavage of the same chimeric ribo/2′-*O*-methylribo oligonucleotides with RNase T1 are 10^5-fold higher than k_{cat} for *pep*-**9** (see Table 1).

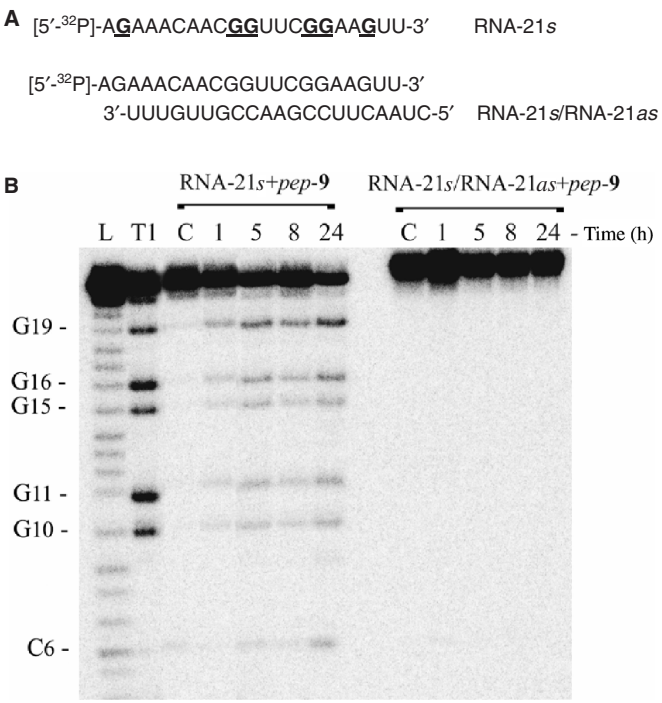

Figure 3. Cleavage of single-stranded and double-stranded RNA substrates with *pep*-**9**. (**A**) Sequence of oligoribonucleotide RNA-21*s* and RNA-21*s*–RNA-21*as* duplex. (**B**) Analysis of RNA-21s and RNA-21*s*–RNA*as* duplex cleavage by *pep*-**9**. Autoradiograph of 12% polyacrylamide/8 M urea gel. Lane L and T1—imidazole ladder and partial RNA digestion in the presence of RNase T1, respectively. Lanes C—RNA-21*s* was incubated in the absence of *pep*-**9** for 24 h. Lanes 1, 5, 8 and 24—[5′-^{32}P]-RNA-21*s* or duplex (10^{-7} M) were incubated in the presence of *pep*-**9** (10 μM) at 37°C for 1, 5, 8 and 24 h. Positions of RNA cleavage by the conjugates and RNase T1 are shown on the left.

pH profile of ribonuclease activity and cleavage specificity of the conjugate pep-9

To elucidate the possible mechanism of RNA cleavage by the conjugate *pep*-**9** and to determine the range of conditions under which *pep*-**9** exhibits the highest ribonuclease activity, we studied pH profile of RNA-96 cleavage by *pep*-**9**. For this purpose, cleavage of RNA-96 was carried out in one of the following buffers with overlapping pH values: sodium acetate–CH_3COOH (pH 3.7–5.0), MES-NaOH (pH 5.0–6.8); Tris-HCl (pH 7.0–9.0); and bis-Tris-propane-HCl (pH 7.0–9.5) (Figure 4). It is seen that pH profile for RNase T1 is bell shaped: RNase T1 displays the highest activity within the pH interval 5.5–6.8 with a maximum at pH 6.0 under the conditions used. The pH profile for RNase T1 obtained using dinucleotide substrate is also bell shaped, but without well-defined optimum (29). The decrease of efficiency of RNA-96 cleavage by RNAse T1 at subacid and subalkali pH is more pronounced in the case of long substrate RNA-96 (96 nt long) than in the case of dinucleotide substrate.

The pH profile for conjugate *pep*-**9** is a half-bell shaped. Conjugate *pep*-**9** displayed the highest activity within the

Table 1. Comparison of the k_{cat} values for cleavage of chimeric ribo/2′-*O*-methylribo oligonucleotides: spontaneously, by *pep*-**9** and RNase T1

Ribo-linkage	k_{cat} ($M^{-1}s^{-1}$)		k_{cat} (s^{-1})	
	RNase T1	*pep*-**9**[a]	Spontaneous hydrolysis[b]	Rate enhancement ($k_{cat\_pep\text{-}9}/k_{cat\_nc}$)
G–A	$(1.4 \pm 0.3) \times 10^5$	0.5 ± 0.07	2.8×10^{-8}	1.8×10^7
G–C	$(3.2 \pm 0.3) \times 10^5$	0.5 ± 0.03	2.3×10^{-8}	2.3×10^7
G–G	$(4.9 \pm 0.5) \times 10^5$	1.3 ± 0.3	1.4×10^{-8}	9.4×10^7
G–U	$(2.0 \pm 0.4) \times 10^5$	0.3 ± 0.03	0.95×10^{-8}	3.1×10^7

[a]Assay conditions: [5′-^{32}P]-end-labelled RNA-10_{GrX} (where X = U, A, G or C) at a concentration of 0.1 μM was incubated in the presence of 5 μM *pep*-**9** in 50 mM Tris-HCl buffer, pH 7.0, containing 1 mM EDTA, at 37°C for 10–100 h.
[b]Assay conditions: [5′-^{32}P]-end-labelled RNA-10_{GrX} (where X = U, A, G or C) at a concentration of 0.1 μM was incubated in the absence of any catalyst in 50 mM Tris-HCl buffer, pH 7.0, containing 1 mM EDTA, at 50–80°C for 10 min–10 h. Effective rate constants of spontaneous RNA cleavage at 37°C were obtained by extrapolation to 37°C data of plot ln(k_{cat}) to $1/T$. k_{cat} of non-catalysed reaction is equal to k_{eff}.

pH range from 3.7 to 7.0. With the increase of pH from 7.0 up to 9.5, we observed 10-fold decrease of the cleavage rate. It is noteworthy that within the pH range conjugate *pep*-**9** cleaved RNA only at G–X linkages. Thus, variation of pH did not affect the specificity of RNA cleavage by the conjugate. At pH 7.0, cleavages of G–X linkages located within single-stranded regions were observed (Figure 2B). When pH was decreased from 7.0 to 3.7, a stepwise increase of cleavage efficiency at the sites within stems was observed, whereas cleavage efficiency of single-stranded regions remained unaffected. With the increase of pH above 7.0, both cleavages within double-stranded and single-stranded regions were inhibited. Drop of conjugate activity at alkaline pH can be explained by changes of electrostatic charges both in RNA substrate and in the oligonucleotide of *pep*-**9** that alter interactions within the conjugate.

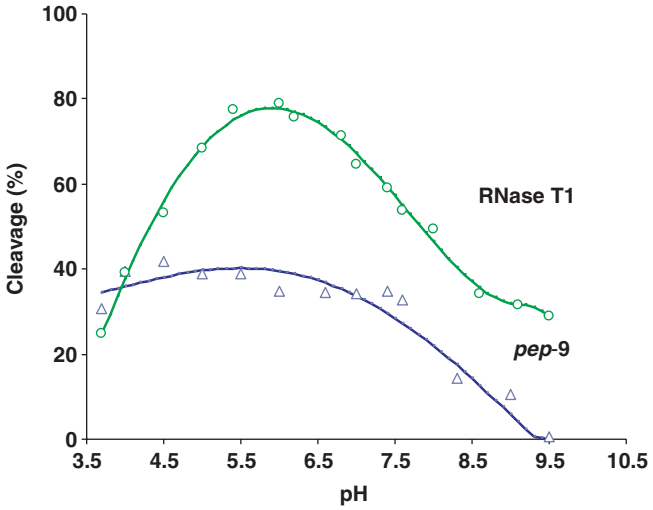

Figure 4. pH profile of RNA-96 cleavage by *pep*-**9** and RNase T1. Buffers are listed in the Materials and methods section. Cleavage activity of *pep*-**9** at various pH was normalized using values of cleavage activity at overlapping pH values.

Effects of monovalent and divalent cations on ribonuclease activity of pep-9

Recently, we demonstrated that activity and cleavage specificity of oligonucleotide–peptide conjugates built of the same peptide NH_2-G(RL)$_4$- and various oligodeoxyribonucleotides is affected by monovalent ions: with increasing concentration, the rate of RNA cleavage at G–X motifs was decreased (up to 20-fold), while the rate of RNA cleavage at Pyr-A motifs was not affected (18). To elucidate the mechanism of RNA cleavage by *pep*-**9**, we studied the effect of monovalent and divalent ions on its ribonuclease activity: RNA substrates (RNA-96 and RNA-10$_{rGG}$) were cleaved by *pep*-**9** at various concentrations of LiCl or $MgCl_2$ (Figure 5).

In the absence of monovalent ions, *pep*-**9** exhibited the highest ribonuclease activity: 90% of RNA-96 was cleaved in 8 h (Figure 5A). Increasing the LiCl concentration up to 500 mM resulted in a 2.5-fold drop in cleavage efficiency. At any LiCl concentration, *pep*-**9** cleaved RNA-96 only at G–X linkages. A similar LiCl concentration profile was observed in the case of short chimeric oligonucleotide RNA-10$_{rGG}$. K^+, NH_4^+ and Cs^+ concentration profiles of RNA-10$_{rGG}$ cleavage by *pep*-**9** (see Figure 1, Supplementary Data) differed insignificantly and showed similar inhibition of reaction at elevated monovalent ion concentration. Analogously, in the presence of Mg^{2+} (5–20 mM), 1.5–3-fold inhibition of cleavage reaction was observed (Figure 5B). It is worth noting that neither monovalent nor divalent ions stimulated cleavage RNA by *pep*-**9**.

Effects of assay conditions on the activity of pep-9: comparison with RNase T1

To characterize the properties of the conjugate *pep*-**9**, we compared the cleavage of RNA-96 by *pep*-**9** and RNase T1 under various conditions. RNA cleavage was

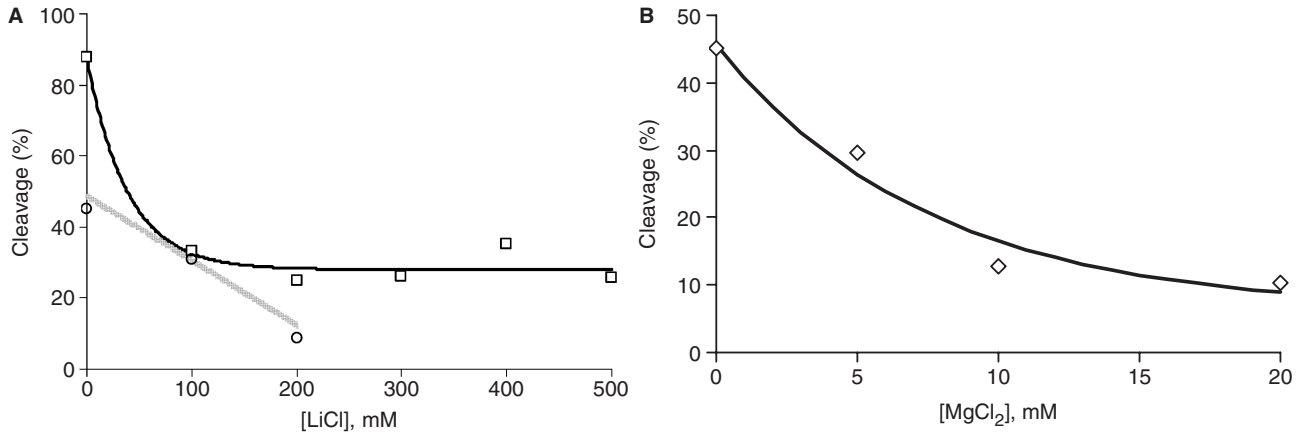

Figure 5. Effect of LiCl (**A**) and $MgCl_2$ (**B**) on ribonuclease activity of *pep*-**9**. Assay conditions. (A) [5′-^{32}P]-RNA-96 (100 μg/ml RNA carrier) or [5′-^{32}P]-RNA-10$_{rGG}$ (10^{-7} M) were incubated in the presence of *pep*-**9** (10 μM) in 50 mM Tris-HCl, pH 7.0, containing 0–500 mM LiCl, 1 mM EDTA, at 37°C for 8 and 52 h for RNA-96 and RNA-10$_{rGG}$, respectively. Solid line and hatched line correspond to RNA-96 and RNA-10$_{rGG}$, respectively. (B) [5′-^{32}P]-RNA-10$_{rGG}$ (10^{-7} M) was incubated in the presence of *pep*-**9** (10 μM) in 50 mM Tris-HCl, pH 7.0, containing 0–20 mM $MgCl_2$, at 37°C for 52 h.

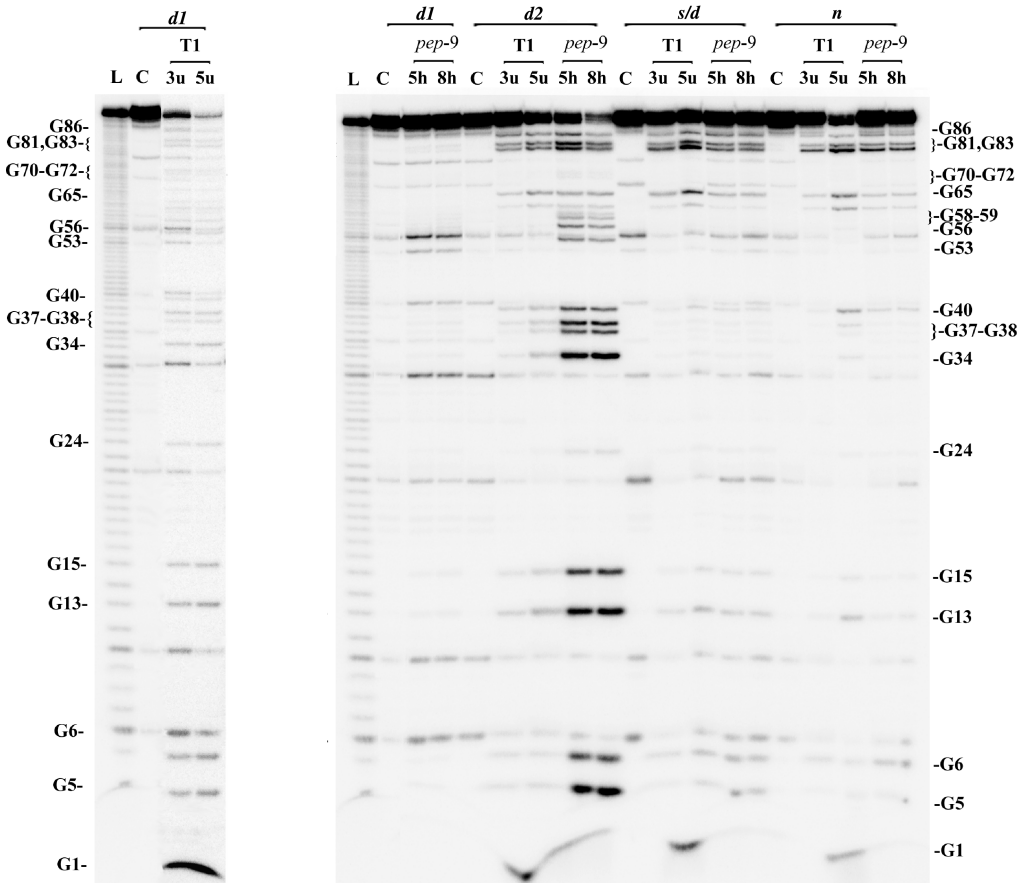

Figure 6. Cleavage of [5′-^{32}P]-labelled RNA-96 by *pep*-**9** and RNase T1 under various conditions. Autoradiograph of 12% polyacrylamide–8 M urea gel. Lanes L—imidazole ladder. Lanes C—RNA incubated in the absence of cleaving agents for 8 h and 15 min, respectively. *pep*-**9** reaction: [5′-^{32}P]-RNA-96 was incubated in the presence of 10 μM *pep*-**9** in buffers *d1*, *d2*, *s*/*d* and *n* at 37°C for 5–8 h. T1-reaction: [5′-^{32}P]-RNA-96 was incubated in the presence of 3–5 U RNase T1 in buffer *d* at 50°C and in buffers *d1*, *d2*, *s*/*d* or *n* at 37°C for 15 min. Buffers are listed in the Materials and methods section. Incubation time, concentration of RNase T1 and experimental conditions are indicated in the top. Location of cleavage sites is shown on the left and right.

carried out under native/physiological conditions (in the presence of potassium and magnesium ions), under semi-denaturing conditions (in the presence of potassium ions only) and denaturing conditions: *d* (6 M urea, 25 mM sodium citrate, pH 4.5–4.8, 1 mM EDTA, at 55°C); *d1* (6 M urea, 50 mM Tris-HCl, pH 7.0, 1 mM EDTA at 37°C) and *d2* (50 mM Tris-HCl, pH 7.0, 1 mM EDTA at 37°C).

Secondary structure of RNA-96 and positions of the cleavage by *pep*-**9** under various conditions are shown in Figure 2B. Under denaturing conditions in the presence of urea (lanes *d1*, Figure 6) no cleavage at G–X motifs by *pep*-**9** was observed, while some cuts at Pyr-A sequences appeared. Under denaturing conditions *d2* (in the absence of 6 M urea, potassium and magnesium ions), *pep*-**9** cleaves all G–X sequences within RNA-96 (lanes *d2*, *pep*-**9**, Figure 6) and displays the same cleavage pattern as RNase T1 under denaturing conditions *d* (lanes *d*, T1, Figure 6), that are optimal for RNase T1 activity. Under semi-denaturing and physiological conditions, cleavage sites of *pep*-**9** coincide with the sites of cleavage by RNase T1. In the presence of mono- and divalent cations, conjugate *pep*-**9** cleaves RNA-96 only at linkages within loops, junction and regions with unstable secondary structure (hairpin 1, Figure 2B). No cleavages in the stems were observed, apparently due to stabilization of RNA structure by magnesium ions. The obtained data clearly show that the conjugate *pep*-**9** can be considered as a reagent useful for investigation of RNA structure in solution under a wide range of conditions.

Structure–activity relationships of conjugate pep-9

The sequence of oligonucleotide GGATCTCTT was systematically varied to find the nucleotides responsible for the G–X cleavage specificity. Mutated conjugates (see Figure 1 for their structure) contain linker group of three deoxyribose residues introduced between oligonucleotide and peptide parts. Cleavage activity of mutated conjugates was assayed using RNA-96 as a substrate (Figure 7).

The data obtained demonstrate that different modifications of the oligonucleotide sequence affect ribonuclease activity and cleavage specificity exhibited by the conjugate. Conjugate *pep*-**9** cleaved RNA only at G–X linkages under various conditions and even at long

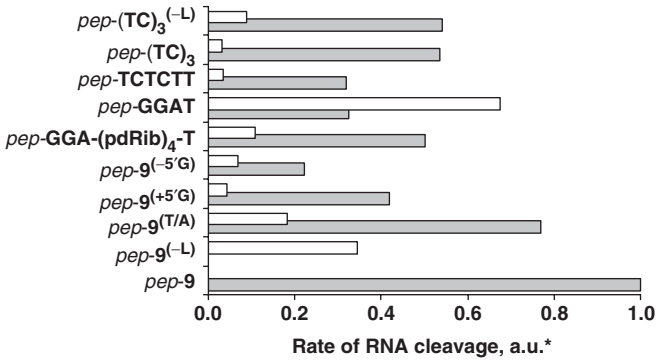

Figure 7. Influence of the oligonucleotide–peptide conjugate structure on cleavage rate and cleavage specificity. Assay conditions: [5′-^{32}P]-RNA-96 was incubated in the presence of 10 μM of the conjugate (except for the conjugates *pep*-**(TC)$_3$** and *pep*-**(TC)$_3^{(-L)}$**) in 50 mM Tris-HCl buffer, pH 7.0, containing 0.2 M KCl, 1 mM EDTA, 100 μg/ml RNA carrier at 37°C for 24 h. Activity of the conjugates *pep*-**(TC)$_3$** and *pep*-**(TC)$_3^{(-L)}$** was assayed at a concentration of 50 μM for 8 h. Rate of RNA cleavage by *pep*-**9** was assumed as 1 (*a.u.—arbitrary unit), and rate of RNA cleavage by other conjugates was calculated relative to *pep*-**9** rate. White and dark bars show the rates of RNA cleavage at Pyr-A and G–X linkages, respectively.

incubation times. Some of the conjugates with altered structure (*pep*-**(TC)$_3$**, *pep*-**9$^{(T/A)}$**, *pep*-**9$^{(+5'G)}$**, *pep*-**GGA-(pdRib)$_4$-T**) also displayed predominant G–X cleavage specificity; however, they cleaved RNA at Pyr-A linkages as well.

Alterations in the 5′-part of the oligodeoxyribonucleotide, for example addition/deletion of guanine residue (conjugates *pep*-**9$^{(+5'G)}$** and *pep*-**9$^{(-5'G)}$**) and deletion of 3-nt fragment (*pep*-**TCTCTT**), were most crucial and resulted in 3–4-fold decrease of G–X cleavage activity. Conjugate *pep*-**(TC)$_3$** demonstrated 1.7-fold decrease of G–X activity and low Pyr-A activity, whereas this conjugate was the more effective G–X ribonuclease as compared to *pep*-**TCTCTT** repeating the main core of oligonucleotide of *pep*-**9**.

Conjugates containing modifications in the 3′-part of oligodeoxyribonucleotide also demonstrated some decrease of ribonuclease activity. Thus, substitution of thymidine by adenine (*pep*-**9$^{(T/A)}$**) as well as deletion of 5-nt fragment at the 3′-end (*pep*-**GGAT**) resulted in 1.4- and 3-fold decrease of G–X activity, respectively, but total ribonuclease activity became unaffected because of the appearance of Pyr-A activity. In the case of conjugate *pep*-**GGAT-(pdRib)$_4$-T**, 2-fold reduction of G–X activity was observed.

Deletion of the linker group of three deoxyribose residues (*pep*-**9$^{(-L)}$**) entirely inhibited G–X activity; this conjugate cleaved RNA at Pyr-A linkages only. Conjugates *pep*-**(TC)$_3$** and *pep*-**(TC)$_3^{(-L)}$** exhibited similar G–X activity, but deletion of the linker group resulted in an increase in the cleavage of Pyr-A linkages.

DISCUSSION

The data obtained show that oligonucleotide–peptide conjugate *pep*-**9** is the first aRNase exhibiting RNase T1-like cleavage activity under a wide range of conditions. The low molecular weight catalyst (*pep*-**9**) discovered is 10^5-fold less active as compared to RNase T1, but it accelerates cleavage at G–X linkages in RNA 10^7–10^8-fold as compared to spontaneous hydrolysis. The unique specificity found is a surprising fact *per se* and requires explanations on which factors (oligonucleotide or/and peptide sequence, conjugate structure, etc.) provide for this specificity.

The conjugate *pep*-**9** functionally mimics RNase T1. The conjugate *pep*-**9** is a single-stranded guanine-specific ribonuclease exhibiting multiple reaction turnover and yielding cleavage products similar to the products of RNase T1 (17). Cleavage of RNA by the conjugate as well as by RNase T1 displays only moderate temperature dependence (30). This fact as well as the saturation curve of the concentration profile of *pep*-**9** are evidences for the cleavage reaction proceeding within the complex RNA/*pep*-**9**. The affinity of the conjugate to RNA is provided by the peptide moiety and oligonucleotide, which is not complementary to RNA substrate, is not involved in binding with RNA. This allows us to postulate *pep*-**9** as an artificial enzyme with aptamer-like peculiarities.

Analysis of structure–function relationships in the conjugate *pep*-**9** clearly shows that any alterations of oligonucleotide sequence and length in *pep*-**9** and deletion of the linker group result in the loss of ribonuclease activity and the appearance of Pyr-A cleavage specificity; thus, the sequence of nonadeoxyribonucleotide GGATCTCTT is obligatory for the conjugate to exhibit G–X specificity. The importance of the linker group between oligonucleotide and peptide parts of the conjugate correlate with the data published in (18). It was found that two or three nucleotides adjacent to the peptide serve as a linker, providing a turn of oligonucleotide around the peptide and facilitating intramolecular oligonucleotide and peptide interactions.

It is known that arginine is a multiple-donor amino acid that can form a number of specific hydrogen bonds with nucleotides (31). The ability of arginine to form hydrogen bonds with DNA/RNA nucleobases within DNA(RNA)–protein complexes decreases in order G>T>A>C (31,32). These properties can be important not only for the interaction of the peptide $(LR)_4$-G with guanine residues in RNA, but also for the specific intramolecular binding of arginine with guanine residues presented in the conjugate.

Thus, the obtained data let us to suppose existence of some active conformation of the conjugate, which is formed as the result of a set of intermolecular contacts between the oligonucleotide and the peptide parts. Electrostatic contacts play an important role in G–X activity of *pep*-**9**, either by stabilization of an 'active' conjugate conformation and/or by stabilization of RNA (G–X motif)/*pep*-**9** reactive complex. This is suggested by the high activity of *pep*-**9** in the absence of mono- and divalent cations and inhibition of its activity in their presence. High ribonuclease activity of *pep*-**9** under the salt-free conditions is an apparent result of the removal of electrostatic shielding of RNA, which facilitates RNA–*pep*-**9** interaction.

The main question is: how does *pep*-**9** cleave G–X linkages? pH profile did not shed light on the possible mechanism of RNA cleavage by *pep*-**9**. Strong decrease of activity could not be attributed to the pK_a values of amino acids and heterocyclic bases because, in this range of pH, charges of arginine and glycine amide remain constant (pK_a are 12.48 and ~9.7 for guanidinium group and for Gly-amide, respectively) (33), and pK_a values of heterocyclic bases (G, C, A and T) lies in the range 9.4–11.2, depending on sequence (34) and microenvironments (35). The data presented allow us to assume that multipoint contacts formed between *pep*-**9** and guanine residue disrupt its stacking with adjacent nucleobases in RNA chain and change conformation to close to the 'in-line' one. Thus, by a set of hydrogen bonds formed with guanine residue, *pep*-**9** causes conformational changes to ribose phosphate of the guanine residue, followed by self-cleavage of the phosphodiester bond. It worth noting that this type of interaction was never described for guanine nucleotides to date, while this reaction is typical for uridine and cytosine nucleotides.

Thus, we developed aRNase displaying G–X cleavage specificity with a unique structure: a chimeric biopolymer built of nonadeoxyribonucleotide and peptide connected by a linker of three deoxyribose residues. Identification of such a unique catalytic structure capable of specific cleaving at G–X linkages is an evidence for the existence of catalysts with aptamer-like peculiarities displaying other specificities. The study of interactions that provide for the activity of this structure can lead to the elucidation of the principles of recognition topology that can be used to design other molecules with unique properties.

ACKNOWLEDGEMENTS

We acknowledge the group of Dr A. Venyaminova for the synthesis of oligoribonucleotides and Dr V. Koval for mass spectral analysis. This work was supported by RAS programs 'Molecular and cellular biology' and 'Science to medicine', RFBR grants no. 05-04-49109 and 06-04-49263. D.V.S. was the recipient of Euler/DAAD fellowship. Funding to pay the Open Access publication charge was provided by RAS program 'Molecular and cellular biology'.

Conflict of interest statement. None declared.

REFERENCES

1. Richards,F.M., Wyckoff,H.W., Carson,W.D. and Allewell,N.M. (1971) Protein structure, ribonuclease S and nucleotide interactions. *Cold Spring Harb. Symp. Quant. Biol.*, **36**, 35–43.
2. Kurachi,K., Davie,E.W., Strydom,D.J., Riordan,J.F. and Vallee,B.L. (1985) Sequence of the cDNA and gene for angiogenin, a human angiogenesis factor. *Biochemistry*, **24**, 5494–5499.
3. Liao,Y.D. (1992) A pyrimidine-guanine sequence-specific ribonucleases from *Rana catesbeiana* (bullfrog) oocytes. *Nucleic Acids Res.*, **20**, 1371–1377.
4. Ardelt,W., Mikulski,S.M. and Shogen,K. (1991) Amino acid sequence of an anti-tumor protein from *Rana pipiens* oocytes and early embryos. *J. Biol. Chem.*, **266**, 245–251.
5. Pace,C.N., Heinemann,U., Hahn,U. and Saenger,W. (1991) Ribonuclease T1: structure, function and stability. *Angew. Chem.*, **30**, 343–360.
6. Vassylyev,D.G., Katayanagi,K., Ishikawa,K., Tsujimoto-Hirano,M., Danno,M., Pahler,A., Matsumoto,O., Matsushima,M., Yoshida,H. *et al.* (1993) Crystal structures of ribonuclease F1 of *Fusarium moniforme* in its free form and in complex with 2′GMP. *J. Mol. Biol.*, **230**, 979–996.
7. Uchida,T., Arima,T. and Egami,F. (1970) Specificity of RNase U2. *J. Biochem. (Tokyo)*, **67**, 91–102.
8. Hubner,B., Haensler,M. and Hahn,U. (1999) Modification of ribonuclease T1 specificity by random mutagenesis of the substrate binding segment. *Biochemistry*, **38**, 1371–1376.
9. Ushijima,K. and Takaku,H. (1998) Site-specific cleavage of tRNA by imidazole and/or primary amine groups bound at the 5′-end of oligodeoxyribonucleotides. *Biochim. Biophys. Acta*, **1379**, 217–223.
10. Hovinen,J., Guzaev,A., Azhayev,A. and Lonnberg,H. (1995) Imidazole tethered oligodeoxyribonucletides: synthesis and RNA cleaving activity. *J. Org. Chem.*, **60**, 2205–2209.
11. Reynolds,M.A., Beck,T.A. and Arnold,L.J. (1996) Antisense oligonucleotide containing an internal, non-nucleotide-based linker promote site-specific cleavage of RNA. *Nucleic Acids Res.*, **24**, 760–765.
12. Bashkin,J.K., Frolova,E.I. and Sampath,U.S. (1994) Sequence-specific cleavage of HIV mRNA by a ribozymes mimic. *J. Am. Chem. Soc.*, **116**, 5981–5982.
13. Endo,M., Hirata,K., Ihahra,T., Sueda,S., Takagi,M. and Komiyama,M. (1996) RNA hydrolysis by the cooperation of carboxylate ion and ammonium. *J. Am. Chem. Soc.*, **118**, 5478–5479.
14. Dock-Bregeon,A.C. and Moras,D. (1987) Conformational changes and dynamics of tRNAs: evidence from hydrolysis pattern. *Cold Spring Harb. Symp. Quant. Biol.*, **52**, 113–121.
15. Tung,C.H., Wei,Z., Leibowits,M.J. and Stein,S. (1992) Design of peptide-acridine mimics of ribonuclease activity. *Proc. Natl Acad. Sci. USA*, **89**, 7114–7118.
16. Mironova,N.L., Pyshnyi,D.V., Ivanova,E.M., Zarytova,V.F., Zenkova,M.A., Gross,H.J. and Vlassov,V.V. (2002) Sequence-specific cleavage of the target RNA with oligonucleotide-peptide conjugates. *Russ. Chem. Bull.*, **51**, 1177–1186.
17. Mironova,N.L., Pyshnyi,D.V., Ivanova,E.M., Zenkova,M.A., Gross,H.J. and Vlassov,V.V. (2004) Covalently attached oligodeoxyribonucleotides induce RNase activity of a short peptide and modulate its base specificity. *Nucleic Acids Res.*, **32**, 1928–1936.
18. Mironova,N.L., Pyshnyi,D.V., Shtadler,D.V., Procudin,I.V., Boutorine,Y.I., Ivanova,E.M., Zenkova,M.A. and Vlassov,V.V. (2006) G-specific RNA-cleaving conjugates of short peptides and oligodeoxyribonucleotides. *J. Biomol. Struct. Dyn.*, **23**, 591–602.
19. Pyshnyi,D.V., Repkova,M.N., Lokhov,S.G., Ivanova,E.M., Venyaminova,A.G. and Zarytova,V.F. (1997) Artificial ribonuclease. 1. Site-directed RNA cleavage by 5′-peptidyloligodeoxyribonucleotides containing arginine and leucine residues. *Bioorgan. Khim. (Russian)*, **23**, 497–504.
20. Mironova,N.L., Pyshnyi,D.V., Ivanova,E.M., Zenkova,M.A., Gross,H.J. and Vlassov,V.V. (2002) Artificial ribonucleases: oligonucleotide-peptide conjugates cleaving GpX and PypA sequences in RNA. *Dokl. Biochem. Biophys.*, **385**, 196–200.
21. Mironova,N.L., Boutorine,Y.I., Pyshnyi,D.V., Ivanova,E.M., Zenkova,M.A. and Vlassov,V.V. (2004) Ribonuclease activity of the peptides with alternating arginine and leucine residues conjugated to tetrathymidilate. *Nucl. Nucleic Acids*, **23**, 885–890.
22. Zarytova,V.F., Ivanova,E.M., Yarmoluk,S.N. and Alekseeva,I.V. (1988) Synthesis of oligonucleotidil-(5′-N)-peptides containing arginine. *Biopolymers Cell (in Russian)*, **1**, 220–222.
23. Mironova,N.L., Pyshnyi,D.V., Stadler,D.V., Zenkova,M.A. and Vlassov,V.V. Oligonucleotide-peptide conjugate capable of cleaving phosphodiester bonds of RNA in 5′-GpN-3′ motives. Russian patent 2006109836, issued 23 March 2006.
24. Silberklang,M., Gillum,A.M. and RhajBhandary,U.L. (1979) Use of in vitro ^{32}P labeling in the sequence analysis of nonradioactive tRNAs. *Methods Enzymol.*, **59**, 58–109.
25. Vlasov,A.V., Vlasov,V.V. and Giege,R. (1996) RNA hydrolysis catalysed by imidazole as a reaction for studying the secondary structure of RNA and complexes of RNA with oligonucleotides. *Dokl. Acad. Nauk.*, **349**, 411–413.

26. Donis-Keller,H., Maxam,A.M. and Gilbert,W. (1977) Mapping adenines, guanines, and pyrimidines in RNA. *Nucleic Acids Res.*, **4**, 2527–2538.
27. Ting,R., Thomas,J.M., Lermer,L. and Perrin,D.M. (2004) Substrate specificity and kinetic framework of a DNAzyme with an expanded chemical repertoire: a putative RNase A mimic that catalyses RNA hydrolysis independent of a divalent metal cation. *Nucleic Acids Res.*, **32**, 6660–6672.
28. Isel,C., Ehresmann,C., Keith,G., Ehresmann,B. and Marquet,R. (1995) Initiation of reverse transcription of HIV-1: secondary structure of the HIV-1 RNA/tRNA(3Lys) (template/primer). *J. Mol. Biol.*, **247**, 236–250.
29. Osterman,H.L., and Walz,F.G.Jr. (1978) Subsites and catalytic mechanism of ribonuclease T1: kinetic studies using GpA, GpC, GpG, and GpU as substrates. *Biochemistry*, **17**, 4124–4130.
30. Mironova,N.L. (2003) Catalysts of RNA cleavage – peptidilologo-nucleotides and organic compounds involving basic amino acids and cation structures. *PhD Thesis*. Institute of Chemical Biology and Fundamental Medicine SB RAS.
31. Luscombe,N.M., Laskowski,R.A. and Thornton,J.M. (2001) Amino acid–base interactions: a three-dimensional analysis of protein–DNA interactions at an atomic level. *Nucleic Acids Res.*, **29**, 2860–2874.
32. Cheng,A.C., Chen,W.W., Fuhramann,C.N. and Frankel,A.D. (2003) Recognition of nucleic acid bases and base-pairs by hydrogen bonding to amino acid side-chains. *J. Mol. Biol.*, **327**, 781–796.
33. Dawson,R., Elliott,D., Elliott,U. and Jones,K. (1986) *Data for Biochemical Research*. 2nd edn. Clarendon Press, Oxford, pp. 15–21.
34. Acharya,S., Barman,J., Cheruku,P., Chatterjee,S., Acharya,P., Isaksson,J. and Chattopadhyaya,J. (2004) Significant pKa perturbation of nucleobases is a intrinsic property of the sequence context in DNA and RNA. *J. Am. Chem. Soc.*, **126**, 8674–8681.
35. Acharya,P. and Chattopadhyaya,J. (2005) Electrostatic cross-modulation of the pseudoaromatic character in single-stranded RNA by nearest-neighbor interaction. *Pure Appl. Chem.*, **77**, 291–311.